ORIGINAL ARTICLE

PIRL1 and *PIRL9*, encoding members of a novel plant-specific family of leucine-rich repeat proteins, are essential for differentiation of microspores into pollen

Nancy R. Forsthoefel · Thuy P. Dao ·
Daniel M. Vernon

Abstract Plant intracellular Ras-group-related leucine-rich repeat proteins (PIRLs) are a plant-specific class of leucine-rich repeat (LRR) proteins related to animal and fungal LRRs that take part in developmental signaling and gene regulation. As part of a systematic functional study of the *Arabidopsis thaliana PIRL* gene family, T-DNA knockout mutants defective in the closely related *PIRL1* and *PIRL9* genes were identified and characterized. *Pirl1* and *pirl9* single mutants displayed normal transmission and did not exhibit an obvious developmental phenotype. To investigate the possibility of functional redundancy, crosses to generate double mutants were carried out; however, *pirl1;pirl9* plants were not recovered. Reciprocal crosses between wild type and *pirl1/PIRL1;pirl9* plants, which produce 50% *pirl1;pirl9* gametophytes, indicated male-specific transmission failure of the double-mutant allele combination. Scanning electron microscopy and viability staining showed that approximately half of the pollen produced by *pirl1/PIRL1;pirl9* plants was inviable and severely malformed. Tetrad analyses with *qrt1* indicated that pollen defects segregated with the double-mutant allele combination, thus demonstrating that *PIRL1* and *PIRL9* function after meiosis. Pollen development was characterized with bright field, fluorescence, and transmission electron microscopy. *Pirl1;pirl9* mutants stopped growing as microspores, failed to initiate vacuolar fission, aborted, and underwent cytoplasmic degeneration. Development consistently arrested at the late microspore stage, just prior to pollen mitosis I. Thus, *PIRL1* and *PIRL9* have redundant roles essential at a key transition point early in pollen development. Together, these results define a functional context for these two members of this distinct class of plant LRR genes.

Abbreviations

DAPI	4′,6-Diamidino-2-phenylindole
LRR	Leucine-rich repeat
PIRL	Plant intracellular Ras-group-related LRR protein
RT-PCR	Reverse transcription PCR
SEM	Scanning electron microscopy
TEM	Transmission electron microscopy

Introduction

Leucine-rich repeat proteins (LRRs) constitute a large and widespread superfamily found in all eukaryotes (Kobe and Deisenhofer 1994; Kajava 1998). Their defining feature is their namesake domain composed of short, tandemly repeated leucine-rich motifs, each 18–29 amino acids in length. Differences in length and consensus sequence of the unit motif form the basis for classification of LRRs within the superfamily (Claudianos and Campbell 1995; Kajava 1998). While found on diverse proteins, LRR domains serve a common purpose, forming platforms that mediate specific protein–protein interactions important for function (Kobe and Deisenhofer 1994; Kobe and Kajava 2001).

N. R. Forsthoefel · T. P. Dao · D. M. Vernon (✉)
Program in Biochemistry, Biophysics and Molecular Biology, Department of Biology, Whitman College, 345 Boyer Avenue, Walla Walla, WA 99362, USA
e-mail: vernondm@whitman.edu

Many LRR proteins take part in cell signaling pathways, often in developmental contexts. One example for this is the "Ras-Group" LRRs found in animals and fungi (Claudianos and Campbell 1995; Buchanan and Gay 1996). Some members of this class are directly involved in Ras-mediated signal transduction, such as *C. elegans* SUR8 and human ERBIN, which mediate Ras interactions with larger regulatory complexes (Sieburth et al. 1998; Sternberg and Alberola-Ila 1998; Li et al. 2000; Dai et al. 2006), and mammalian Rsu/Rsp-1, which can suppress Ras-mediated transformation (Cutler et al. 1992; Dougherty et al. 2008). Another Ras-group LRR, FLI-1, binds transcription complexes and takes part in hormone-induced chromatin remodeling in mammals (Lee et al. 2004; Jeong et al. 2009), indicating that Ras-group LRRs may have diverse biochemical functions.

In plants as in other eukaryotes, LRRs function in a wide range of developmental processes (Vernon and Forsthoefel 2002). Prominent examples of major plant LRR families include the LRR-receptor kinases, which feature extracellular N-terminal LRR domains important for ligand recognition in numerous developmental and physiological pathways (Morris and Walker 2003; Dievart and Clark 2004; Morillo and Tax 2006; De Smet et al. 2009). Some F-box proteins that mediate signal-responsive protein degradation also feature LRR domains (Hellmann and Estelle 2002; Somers and Fujiwara 2009), and two different classes of disease resistance proteins, NBS-LRRs and *cf*-type receptors, feature LRR domains involved in pathogen recognition or response (Fluhr 2001; Belkhadir et al. 2004; McHale et al. 2006; Eitas and Dangl 2010).

Plant intracellular Ras-group-related LRRs (PIRLs) are a small protein class featuring a conserved internal LRR domain comprised of unit motifs most closely related to those found in animal and fungal Ras-group LRR proteins (Forsthoefel et al. 2005). The LRR domains are flanked by divergent hydrophilic terminal regions. PIRLs are a plant-specific protein family: no close homologs with similarity beyond the LRR motifs are identified in other eukaryotes. Beyond the LRR domain, PIRLs lack other features found in some major LRR classes in plants, such as signal or transmembrane sequences, kinase domains, or nucleotide binding sequences (Morris and Walker 2003; Morillo and Tax 2006; McHale et al. 2006, Eitas and Dangl 2010). Based on this combination of features, PIRLs constitute a novel class of plant LRRs related to Ras-group proteins by virtue of their LRR motif sequence. The *Arabidopsis thaliana* genome contains nine *PIRL* genes that fall into three subfamilies, the largest of which, sub-family I, consists of *PIRL1*, *PIRL2*, *PIRL3*, and *PIRL9*. Within this group, *PIRL1* and *PIRL9* are the most closely related, with products sharing 77% amino acid identity. These sequence relationships and the widespread expression of *PIRL*

subfamily I mRNAs (Forsthoefel et al. 2005) make for potential functional redundancy between these genes.

The structural relationship between PIRLs and Ras-group LRRs suggests potential functions for the *PIRL*s in plant development, and we have undertaken a systematic reverse genetic investigation of Arabidopsis *PIRL*s using T-DNA knockout mutants to investigate this hypothesis. Here, we report that the *PIRL1* and *PIRL9* genes are genetically redundant and required for differentiation of microspores into pollen, a plant-specific developmental process crucial for reproduction. Loss of *PIRL1* and *PIRL9* gene functions results in transmission failure specifically through the male gametophyte due to arrest of microspore development just prior to the first pollen mitosis. These results establish that *PIRL1* and *PIRL9* have redundant functions essential at a key transition point early in the development of the male gametophyte, and they provide the first functional information on this novel class of plant LRR proteins.

Materials and methods

Plant materials

Plants were grown on soil from seed under 16 h light/8 h dark conditions as described by Cushing et al. (2005). In initial work with prospective T-DNA-insertion lines from the Wisconsin collections (Sussman et al. 2000), seeds were plated in culture on Murashige and Skoog medium supplemented with 1% sucrose, following surface sterilization as previously described (Vernon and Meinke 1994; Vernon et al. 2001), in the presence of 50 μg mL^{-1} kanamycin, to identify plants with T-DNA inserts.

Mature pollen for viability staining or scanning electron microscopy (SEM) was collected on slides from open flowers from plants that had been previously genotyped by PCR (see genetic analysis, below). *Pirl1*/*PIRL1*;*pirl9* plants, which produce 50% double-mutant pollen, were used for analysis of the *pirl1*;*pirl9* pollen phenotypes unless otherwise indicated in "Results". For characterization of microspore and pollen development, developing flowers were excised from wild-type controls or previously genotyped plants segregating for single- or double-mutant pollen, and subjected to clearing or anther-squashing treatments as described below.

Mutant identification, genetics, and molecular characterization

Sequence data for *PIRL* mRNA and proteins were previously deposited in Genbank and protein databases (Forsthoefel et al. 2005), and the gene nomenclature is registered at

TAIR (http://www.arabidopsis.org). Nucleotide accessions: AY849571 (*PIRL1*); AY849579 (*PIRL9*). Protein accessions: AAW57410 (PIRL1) and AAW57418 (PIRL9). TAIR Atg loci designations: At5g05850 (*PIRL1*) and At3g11330 (*PIRL9*).

The *pirl1-1* and *pirl9-1* knockout lines were identified among pooled lines provided by the University of Wisconsin Knockout Facility, using the prescribed PCR screening and Southern blot strategy (Krysan et al. 1999; Sussman et al. 2000). T-DNA-specific primers were those dictated by the knockout facility protocols: JL202 (left-border specific), CATTTTATAATAACGCTGCGGACA TCTAC; XR2 (right-border specific), TGGGAAAACCT GGCGTTACCCAACTTAAT. Gene-specific primers for knockout screens were: AGATCATTCTCAAGCCCATA AAACATTTG (*PIRL1*-RG, forward), GCAGGAAAACT CAAGACTGAAGATCACTT (*PIRL1*-RG, reverse), AA CTTGACATCAGAGAAAACGCAGAGAAG (*PIRL9*-RG, forward), and AAACGAGAAATTTCAACCTCTTT GGATTC (*PIRL9*-RG, reverse). Plants containing the mutant alleles were sequentially backcrossed to wild type (ecotype Wassilewskija, WS) three times prior to phenotype analysis or further genetic experiments.

Both *pirl1-2* alleles and the *pirl9-2* allele were identified in the publically available sequence-indexed Salk insertion mutant collection (Alonso et al. 2003; ecotype Columbia), and seeds were obtained from the Arabidopsis Biological Resource Center (ABRC, Ohio State University). Salk designations for these lines were S072332 and S146770 for *PIRL1* and *PIRL9*, respectively. Detailed information on T-DNA insert positions and orientations for these alleles is available at the Arabidopsis Information Resource (TAIR, http://www.arabidopsis.org). T-DNA insert locations in all lines were confirmed by PCR of T-DNA–plant junction fragments using genomic DNA preparation as described by Tax and Vernon (2001) and PCR as described by Cushing et al. (2005). Primers used for T-DNA–plant junction amplification were the LBb1 T-DNA left-border primer (GCGTGGACCGCTTGCTGCAACT) in combination appropriate gene-specific primers: *PIRL1* forward primer, CCTCAATCTCCCAATCGTCTCTTCC; reverse primer, GCAGCGGCAGGAAAACTCAAGAC; *PIRL9* forward primer, TCGTCACTCAGATGCCTCAC; reverse primer, CACCTTCCTTCACCACTTCC. Specificity and product identity for these gene-specific primers had been previously verified by product sequencing (Forsthoefel et al. 2005).

Genotyping to identify mutant homozygotes, heterozygotes, and carriers of both mutations was done by PCR, using gene-specific forward and reverse primer combinations to detect wild-type alleles, and T-DNA:*PIRL* primer combinations to detect the presence of mutant alleles. DNA was isolated from individual leaves as described by Tax and Vernon (2001), and subjected to PCR as described by Cushing et al. (2005), using the primers described above for verification of T-DNA insert location. Analysis of *pirl1* and *pirl9* mutant allele segregation and transmission was done using this genotyping procedure on populations of seedlings produced by either self-fertilization or by controlled crosses between genotypes, as indicated for each experiment in the "Results" section.

Crosses to *qrt1* were carried out by crossing *pirl1;pirl9/ PIRL9* individuals to homozygous *qrt1* plants grown from *qrt1* seed (Preuss et al. 1994) obtained from the ABRC (Ohio State University). The *pirl* parent served as female for these crosses to insure transmission of both mutant alleles to 50% of the F1s. F1 individuals were genotyped by PCR to identify individuals heterozygous for both *pirl* knockout alleles. These plants were then selfed, F2 seed collected, and individuals homozygous for *qrt1* (25%) identified in the F2 by visual screening of pollen. *Qrt1* individuals were subjected to PCR genotyping to identify *qrt1;pirl1/PIRL1;pirl9* plants for pollen analysis. Pollen tetrads were subjected to Alexander's staining, then quantified by bright field microscopy to determine the percentage of aborted pollen and quantify its distribution in tetrads.

Sequence analyses and amino acid sequence predictions were done with empirically determined cDNA sequences (Forsthoefel et al. 2005), using MacVector software (Accelrys, San Diego, CA, USA). Protein domain predictions were carried out using the Simple Modular Architecture Research Tools (http://smart.embl-heidelberg.de/; Letunic et al. (2009). RNA isolation and RT-PCR to determine null status of mutant alleles were carried out as described by Cushing et al. (2005), using the gene-specific forward and reverse primer pairs described above. Reactions were carried out for 35 cycles (94°C for 45 s, 58°C for 60 s, and 72°C for 120 s). PCR results were visualized on 1% agarose gels.

Pollen development and microscopy

For pollen SEM, mature flowers from 3–10 PCR-genotyped plants of each genotype were collected and dried for at least 2 days. Pollen was transferred to a stub and sputter-coated with gold–palladium at 18 mA for 120 s under partial vacuum with Argon using a Pelco Sputter Coater Model 3 (Ted Pella, Redding, CA, USA). Samples were viewed in a JSM-T300 scanning electron microscope (JEOL USA, Peabody, MA, USA), and images were collected on film, or they were viewed and digitally imaged using an FEI Quanta200 scanning electron microscope with variable vacuum and Peltier cold stage capabilities (FEI, Hillsboro, OR, USA).

Viability staining was carried out using a 1:50 dilution of Alexander's stain stock solution [10 mL 95% ethanol,

5 mL 1% malachite green in 95% ethanol, 5 g of phenol, 5 mL 1% acid fuchsin in H_2O, 0.5 mL 1% orange G in H_2O, 2 mL glacial acetic acid, 25 mL glycerol, and 50 mL H_2O (Alexander 1969; Johnson-Brousseau and McCormick 2004)]. For samples, plants were genotyped using the PCR protocol described above, and stained according to the method of Henry et al. (2005), using 3–5 flowers excised from 3–9 separate plants of each indicated genotype. Pollens were observed by bright field microscopy, and staining was quantified manually.

For microscopy of developing microspores and pollen, flowers of various developmental stages were excised from *pirl1/PIRL1;pirl9* plants at the pedicel, dissected to expose anthers and treated as follows. For fluorescence microscopy, anthers were removed, gently squashed under coverslips in 25 µl 4′,6-diamidino-2-phenylindole (DAPI) solution [0.1 M sodium phosphate (pH 7), 1 mM EDTA, 0.1% Triton X-100, 0.5 µg mL^{-1} DAPI, high grade], and viewed by bright field and UV epi-illumination on a Leica DMIRB microscope equipped with a Coolsnap camera (Photometrics, Tucson, AZ, USA). For callose staining, anthers were placed on slides in 25 µl 0.1% aniline blue in 0.1 M phosphate buffer (pH 8.6) and similarly viewed by bright field and UV epi-illumination. Anther developmental stages were designated according to the conventions described by Sanders et al. (1999). Histological and transmission electron microscopy (TEM) samples were prepared by the Franceschi Microscopy and Imaging Center at Washington State University (Pullman, WA, USA). Inflorescence buds were excised from PCR-genotyped *pirl1/PIRL1;pirl9* plants segregating for double-mutant microspores. Samples were fixed, dehydrated, and embedded according to Trump et al. (1961), sectioned at 1 µm, and stained for light microscopy with toluidine blue (0.5% in 1% borax) for 0.5–2 min, or for TEM with 2% uranyl acetate for 8 min, followed by Reynolds lead for 8–10 min.

Results

Identification of *pirl1* and *pirl9* T-DNA knockout alleles

PIRL1 and *PIRL9* comprise the most closely related gene pair in the Arabidopsis *PIRL* family. The predicted products have similar domain organization, with a characteristic PIRL LRR region consisting of nine tandem leucine-rich motifs (Forsthoefel et al. 2005), flanked by 204 amino acid N-terminal and 76 amino acid C-terminal regions, both of which are hydrophilic and feature charged residues and some low-complexity sequences (Fig. 1). A potential coiled coil is predicted N-terminal to the leucine-rich
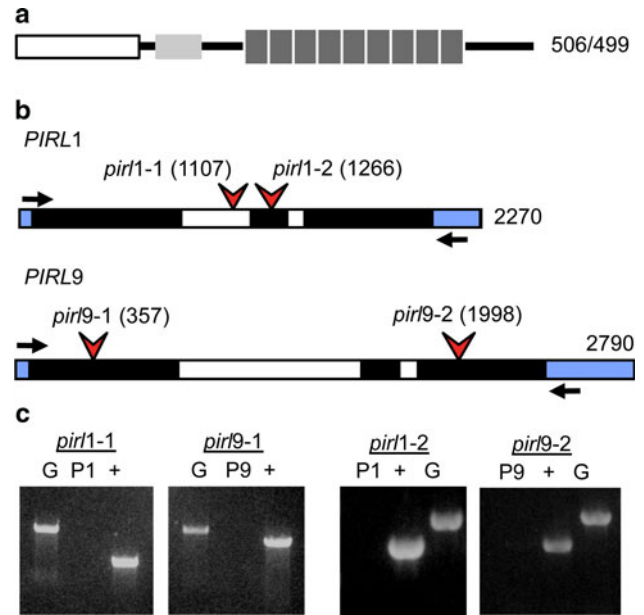

Fig. 1 *PIRL1* and *PIRL9* gene structures, knockout alleles, and predicted protein features. **a** Predicted PIRL1 and PIRL9 protein domain architecture. *Dark boxes* Leu-rich motifs constituting the LRR domain; *white* hydrophilic N-terminal region; *lightly shaded region* predicted coiled-coil domain. Length in amino acids is indicated at *right* (PIRL1/PIRL9). Amino acid sequences and alignments for the PIRL protein family have been described previously (Forsthoefel et al. 2005). NCBI protein accessions and TAIR locus designations: PIRL1, AAW57410 and At5g05850; PIRL9, AAW57418 and At3g11330. **b** Gene maps and T-DNA insertion alleles used in this study. Exons are *shaded*, with coding regions in *black*; introns are *white*. Length in nucleotides is indicated at *right*. *Arrowheads* mark confirmed T-DNA insert positions, with insertion site nucleotide positions indicated in *parentheses*. *Black arrows* mark positions of primers used in **c**. **c** Confirmation of knockout status by RT-PCR. PolyA RNA prepared from *pirl1* or *pirl9* single-mutant homozygote seedlings was subjected to RT-PCR to detect the presence of *PIRL* transcripts, and products were resolved on 1% agarose gels. Knockout mutants from which RNA was isolated are indicated above each respective gel. G, genomic PCR product shown as control for primer efficacy; P1 or P9, *PIRL1* or *PIRL9* RT-PCR amplification products (lacking in corresponding homozygous mutants); *plus* amplification of transcripts from the non-disrupted *PIRL* locus, included as positive controls for RT-PCR efficacy

repeats. PIRL1 and PIRL9 are encoded by the unlinked At5g05850 and At3g11330 loci, respectively. The structural annotations of both genes have been empirically confirmed, and mRNAs for both are widely expressed during plant development, based on RNA blots, reverse-transcription PCR (RT-PCR), and Genevestigator data (Forsthoefel et al. 2005; Zimmermann et al. 2004).

Two knockout alleles for each locus were identified using the Wisconsin and Salk Arabidopsis T-DNA insertion mutant collections (Sussman et al. 2000; Alonso et al. 2003). Wisconsin alleles were designated *pirl1-1* and *pirl9-1*, and Salk alleles *pirl1-2* and *pirl9-2*. Gene maps showing T-DNA positions are shown in Fig. 1b. Insert positions were

Table 1 Normal genetic transmission of *pirl1* and *pirl9* single knockout alleles and viability of single-mutant homozygotes

Cross[a]	F1 prediction[b]	F1 genotypes[c]
pirl1-1 +/− × *pirl1-1* +/− (selfed)	25% −/− in F1	15/69 (22%) −/−
pirl1-2 +/− × *pirl1-2* +/− (selfed)	25% −/− in F1	6/22 (30%) −/−
pirl9-1 +/− × *pirl9-1* +/− (selfed)	25% −/− in F1	14/47 (29%) −/−
pirl9-2 +/− × *pirl9-2* +/− (selfed)	25% −/− in F1	6/24 (25%) −/−
pirl1-1 +/− × WT	50% +/− in F1	20/44 (45%) +/−
WT × *pirl1-1* +/−	50% +/− in F1	23/48 (48%) +/−
pirl1-2 +/− × WT	50% +/− in F1	11/23 (48%) +/−
WT × *pirl1-2* +/−	50% +/− in F1	11/19 (58%) +/−
pirl9-1 +/− × WT	50% +/− in F1	13/24 (54%) +/−
WT × *pirl9-1* +/−	50% +/− in F1	21/48 (44%) +/−
pirl9-2 +/− × WT	50% +/− in F1	29/66 (44%) +/−
WT × *pirl9-2* +/−	50% +/− in F1	35/70 (50%) +/−

[a] Crosses using different mutant alleles of each of *pirl1* and *pirl9*, as indicated. *WT* wild type. Top tier: self-fertilization of heterozygotes, demonstrating normal mutant allele transmission and viability of homozygotes in the F1. Bottom tier: reciprocal crosses to WT, demonstrating normal transmission of knockout alleles

[b] Predictions of mutant allele transmission to the F1, based on normal Mendelian transmission and viability of homozygous mutant F1 progeny

[c] F1 seedling genotypes were determined by PCR using gene-specific and gene/T-DNA-specific primer combinations as described in "Materials and methods"

confirmed by PCR and sequencing to verify T-DNA insertion site and structure and to ensure that additional T-DNA-associated chromosomal rearrangements were not present, as is occasionally the case with T-DNA insertion lines (Tax and Vernon 2001). T-DNAs in all alleles were located within *PIRL* transcription units. Mutants were subjected to serial backcrossing to wild type to remove the influence of any potential secondary mutations. RT-PCR was used to confirm knockout status for each of the four mutant alleles using RNA from single-mutant homozygotes. Expression of mRNAs

from disrupted loci was not detected, consistent with the internal location of T-DNA inserts (Fig. 1c).

Genetic analysis reveals a role for *PIRL1* and *PIRL9* in the male gametophyte

Pirl1 and *pirl9* homozygous mutants were recovered routinely and resembled wild type. PCR analysis of mutant allele transmission in F1 progeny of selfed heterozygotes and of heterozygotes crossed to wild type further demonstrated that single-mutant homozygotes are viable, and that the individual knockout alleles exhibit normal segregation and transmission (Table 1). To investigate possible functional redundancy between these related genes, we then attempted construction of double mutants. However, double *pirl1;pirl9* mutants could not be identified in progeny populations of selfed *pirl1/PIRL1;pirl9* or *pirl1;pirl9/PIRL9* plants ($n = 142$; $\chi^2 = 47.3$; $P \gg 0.005$), suggesting lethality or gametophytic transmission failure of the *pirl1;pirl9* mutant combination. The possibility of embryo lethality was ruled out through observation of siliques and developing seeds using established methods for analysis of *embryo-defective* mutants (Meinke 1995; Vernon and Meinke 1994).

To investigate the possibility of gametophytic transmission failure, reciprocal crosses to wild type were carried out with *pirl1/PIRL1;pirl9* plants, which produce 50% *pirl1;pirl9* double-mutant gametophytes. F1 progeny were genotyped by PCR to assess allele transmission; results are shown in Table 2. The *pirl1;pirl9* allele combination was transmitted normally through the female parent, resulting in approximately 50% of F1 progeny containing mutant alleles for both *pirl1* and *pirl9* when wild-type plants were used as pollen donors. However, when *pirl1/PIRL1;pirl9* plants were used as pollen donors, no *pirl1* mutant allele transmission was observed; all F1 progeny contained a wild-type *PIRL1* allele. This male-specific transmission

Table 2 Male-specific gametophytic transmission failure of the *pirl1,pirl9* double-mutant allele combination

Parent genotype[a]	Expected heterozygosity in F1[b]	Observed heterozygotes in F1[c]	χ^2 (P value)[d]
pirl1-1 +/−, *pirl9-1* −/− × WT	24/48 *pirl1* heterozygotes	22/48 (46%)	0.33 (NS)
WT × *pirl1-1* +/−, *pirl9-1* −/−	35/69 *pirl1* heterozygotes	0/69 (0%)	69 (<0.001)
pirl1-2 +/−, *pirl9-2* −/− × WT	23/46 *pirl1* heterozygotes	23/46 (50%)	0 (NS)
WT × *pirl1-2* +/−, *pirl9-2* −/−	24/48 *pirl1* heterozygotes	0/48 (0%)	48 (<0.001)

[a] Reciprocal crosses with wild type (WT), using *pirl1/PIRL1;pirl9* plants as pollen donors or recipients (these plants produce 50% *pirl1;pirl9* double-mutant pollen and 50% *PIRL1;pirl9* single-mutant pollen). For each cross, the female parent is listed first, pollen donor second

[b] Expected values were based on the prediction that if mutant alleles were transmitted normally, ~50% of progeny should receive the *pirl1* knockout allele from the *pirl1/PIRL1;pirl9* parent

[c] F1 seedlings were genotyped by PCR using gene-specific and gene/T-DNA-specific primer combinations, as described in "Materials and methods"

[d] χ^2 values were calculated based on an expected 1:1 ratio of *pirl1/PIRL1* to *PIRL1/PIRL1* F1 genotypes, with significant *P* values indicative of abnormal transmission. NS not significant ($P > 0.05$)

failure was observed with both the *pirl1-1;pirl9-1* and the *pirl1-2; pirl9-2* allele combinations (Table 2), verifying that it was due to *PIRL* gene disruption.

Inviability of *pirl1;pirl9* pollen

The observed *pirl1;pirl9* transmission failure could have been due to a defect in pollen development and viability, or to flaws in subsequent steps of pollen function, such as pollen tube elongation, guidance, or fertilization itself. To investigate the developmental basis of transmission failure, mature pollen produced by wild type and *pirl1/PIRL1;pirl9* plants was examined by SEM. Plants segregating for the double-mutant allele combination produced approximately 50% grossly distorted and shrunken pollen (Fig. 2), a frequency corresponding to the expected meiotic segregation of the *pirl1;pirl9* double-mutant genotype. In contrast, wild-type plants and single-mutant homozygotes produced deformed pollen at much lower frequencies, with single mutants (which generate 100% mutant pollen) only producing 6–8% abnormal pollen (Fig. 2f).

In some Arabidopsis mutants, pollen lethality has been associated with defective exine patterning or synthesis (Paxson-Sowders et al. 2001; Dong et al. 2005; Guan et al. 2008). However, SEM indicated that despite severe morphological defects, exine patterning on the prospective *pirl1;pirl9* pollen resembled that of wild type.

Alexander's staining was used to assess viability of *pirl1;pirl9* mutant pollen. Approximately 42–44% of pollen produced by *pirl1/PIRL1;pirl9* plants was unambiguously aborted based on this staining (Fig. 3), which provides a conservative estimate of pollen viability (Dafini et al. 2005; Baez et al. 2002). This corresponds to the predicted segregation of the double-mutant genotype in pollen produced by such parents. The high frequency of pollen inviability suggested that the pollen transmission failure observed in reciprocal crosses resulted from a highly penetrant defect in pollen development, rather than later defects in pollen tube elongation, guidance, or fertilization.

The *pirl1* and *pirl9* mutations affect pollen development after meiosis

Double-mutant allele transmission and phenotype segregation suggested *pirl1* and *pirl9* act after meiosis. To confirm this, *pirl1* and *pirl9* were crossed into a *qrt1* background (Preuss et al. 1994), and segregation of the pollen-defective phenotype was evaluated in pollen tetrads produced by *qrt1;pirl1/PIRL1;pirl9* individuals. Results are shown in Fig. 4. Tetrads produced by *qrt1* control plants, or *qrt1* plants homozygous for either only *pirl1* or *pirl9*, produced only a background frequency of abnormal pollen, and the rare aborted pollen were observed mainly as single aborted
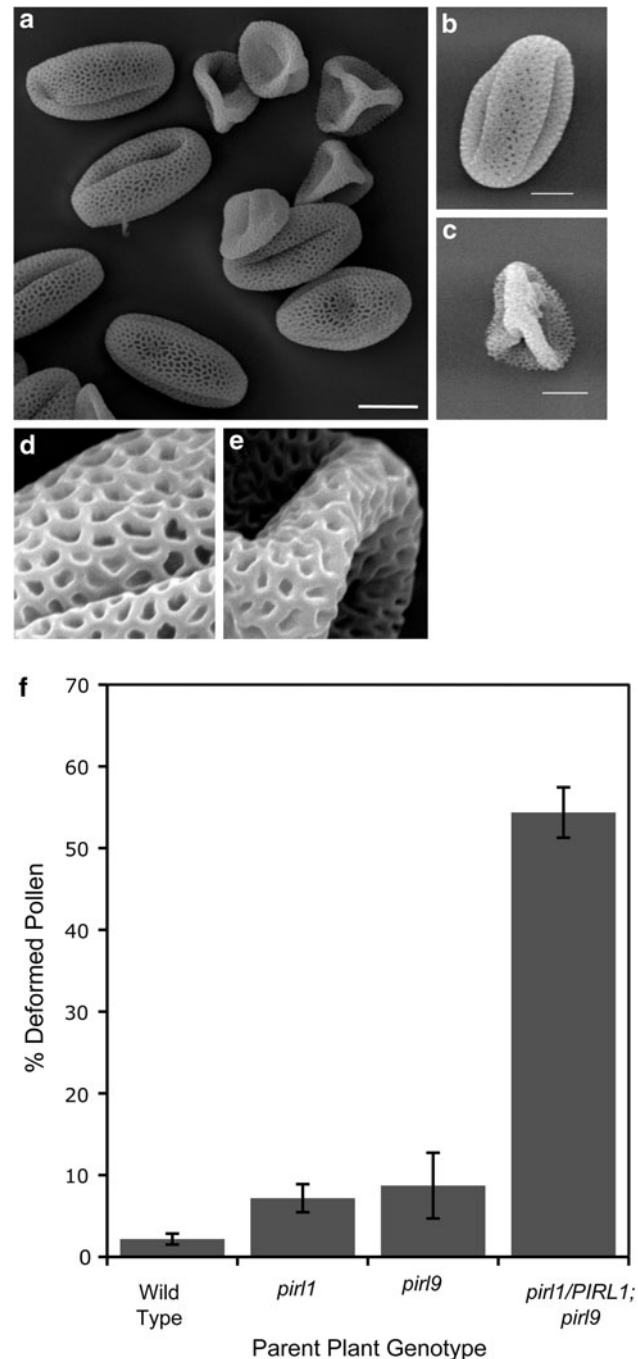

Fig. 2 Severe morphological defects in prospective *pirl1;pirl9* double-mutant pollen. Dehisced pollen was collected from wild type, *pirl* single mutants, or *pirl1/PIRL1;pirl9* plants and viewed by SEM. Plant genotypes were determined by PCR as described in "Materials and methods". **a** Pollen from a *pirl1/PIRL1;pirl9* plant, showing prospective double-mutant pollen segregating with phenotypically normal grains. *Bar* 10 μm. **b, c** Wild type and prospective double-mutant pollen, respectively; *bar* 5 μm. **d, e** Similar exine patterning on wild type (**d**) and prospective double-mutant pollen (**e**), despite morphologic deformity. **f** Frequency of distorted pollen produced by wild type, *pirl* single mutants (which produce 100% single-mutant pollen), and *pirl1/PIRL1;pirl9* plants (which produce 50% *pirl1;pirl9* pollen). Mean values (±SE) derived from 3–10 plants of each genotype are plotted. *n* = 597, 128, 88, 1,341, respectively
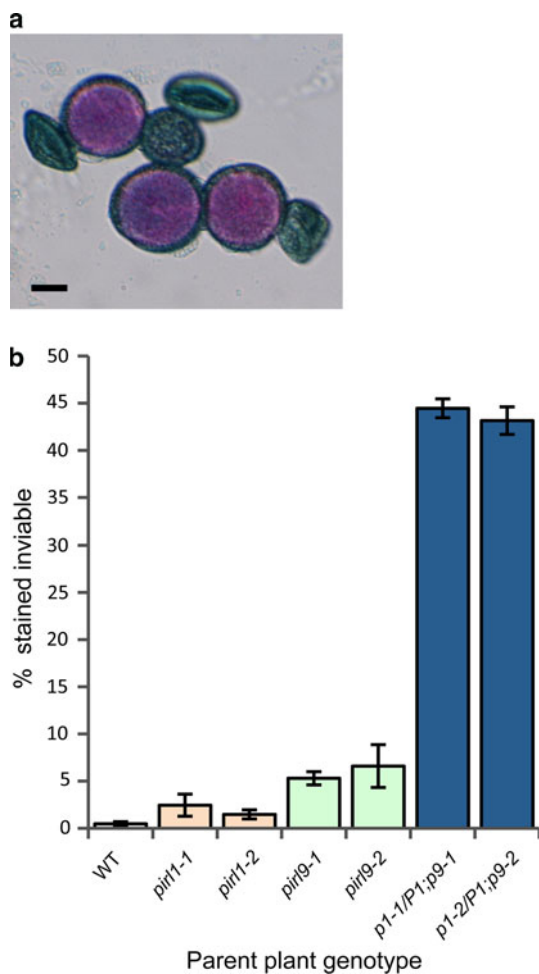
Fig. 3 Inviability of prospective *pirl1*;*pirl*9 double-mutant pollen. Mature pollen from flowers excised from parent plants of indicated genotypes were subjected to Alexander's staining to assess viability. Genotypes were determined by PCR as described in "Materials and methods". Homozygous *pirl1* or *pirl*9 single mutants produce 100% single-mutant pollen, *pirl1*/*PIRL1*;*pirl*9 (*p1*/*P1*;*p9*) plants produce 50% *pirl1*;*pirl*9 double-mutant pollen. **a** Photograph of pollen from a *pirl1*/*PIRL1*;*pirl*9 plant, illustrating segregation of inviable pollen (*blue-green*). *Bar* 10 μm. **b** Quantification of Alexander staining results. Mean values (±SE) derived from 3–10 plants of each genotype are plotted. *n* values: 968, 544, 747, 1,622, 364, 2,378, 1,103, respectively

grains in an occasional tetrad. In contrast, *qrt1*;*pirl1*/*PIRL1*;*pirl*9 plants overwhelmingly produced tetrads with two normal and two aborted pollen grains, consistent with the meiotic segregation of *pirl1*,*pirl9* genotype (Fig. 4b). These results indicated that the *pirl1* and *pirl9* mutations act after meiosis to affect microspore or pollen development.

Arrested growth and differentiation of *pirl1*;*pirl9* microspores

To determine when the *PIRL1* and *PIRL9* genes are first required, we examined pollen development in *pirl1*/
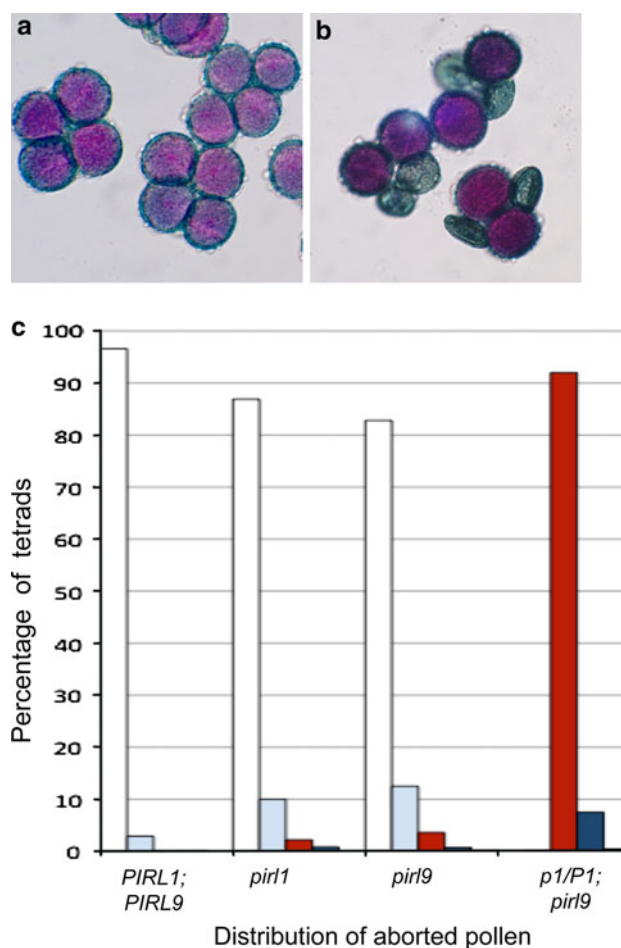

Fig. 4 Post-meiotic segregation of the *pirl1*;*pirl9* mutant phenotype in a *qrt1* background. *pirl1-1* and *pirl9-1* mutant alleles were crossed into *qrt1*, and plants of indicated genotypes were identified in the F2 by PCR as described in "Materials and methods". Segregation of aborted pollen produced by parent plants of each genotype was determined by Alexander's stain. *pirl1*/*PIRL1*;*pirl*9 (*p1*/*P1*;*pirl9*) plants were predicted to produce tetrads with two aborted pollen if the phenotype were caused by post-meiotic expression of the *pirl1*;*pirl9* allele combination. **a** Representative tetrads produced by a *qrt1*;*PIRL1*;*PIRL9* control plant. **b** Tetrads produced by a *qrt1*;*pirl1*/*PIRL1*;*pirl*9 plant that segregates for 50% *pirl1*;*pirl9* pollen. **c** Comparison of the distribution of aborted pollen in tetrads produced by control *qrt1* plants, *pirl1* and *pirl*9 single mutants, and *qrt1*;*pirl1*/*PIRL1*;*pirl*9 plants. *Bar colors* represent tetrads with different numbers of aborted pollen, for each genotype: *white* tetrads with zero aborted pollen; *lightest blue shading* tetrads with one aborted; *medium* (*red*) *shading* tetrads with two aborted; *darkest blue shading* tetrads with three aborted pollen. *n* values, number of tetrads: 411, 346, 468, and 890, respectively

PIRL1;*pirl9* anthers, which segregate 50% for *pirl1*;*pirl9* pollen. Anther sections stained with toluidine blue were examined first to determine when mutants first became morphologically distinct from segregating normal pollen. Results are shown in Fig. 5. Double mutants could not be distinguished from wild-type microspores in tetrads viewed just after meiosis, or in early free microspores. However,
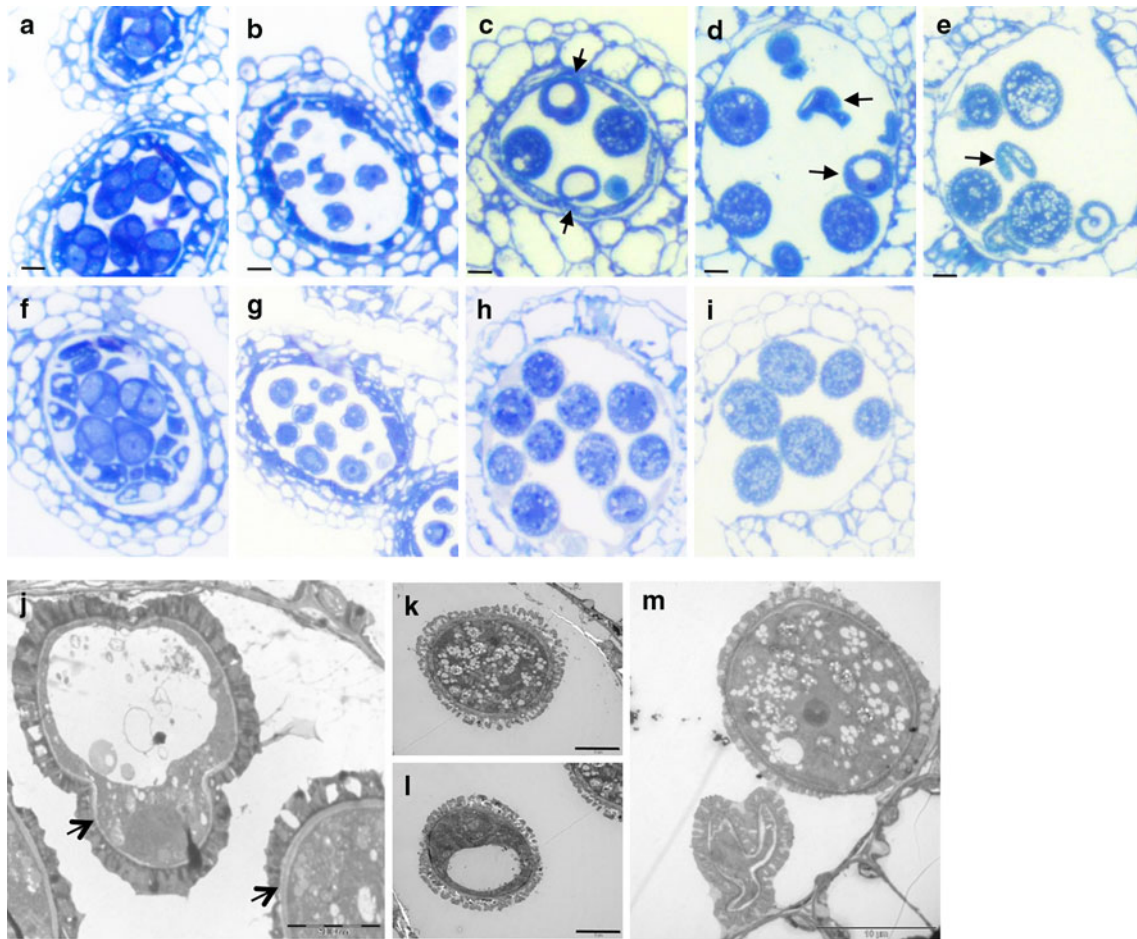
Fig. 5 Arrested development of *pirl1*;*pirl9* microspores. Microspores and pollen at different developmental stages were viewed in anthers from *pirl1/PIRL1*;*pirl9* plants, which produce pollen segregating 50% for the *pirl1*;*pirl9* genotype. *Arrows* mark representative arrested pollen. **a–i** Anther sections stained with toluidine blue and visualized by bright field microscopy. **a–e** Sections of *pirl1/PIRL1*;*pirl9* anthers; *scale bars* 10 μm. **f–i** sections of WT controls from approximately equivalent anther stages, shown at the same scale. Stages were designated as described by Sanders et al. (1999). **a, f** Tetrads just after meiosis; **b, g** free microspores shortly after separation from tetrads, with mutants not yet morphologically distinguishable from normal siblings. **c, h** Locules from mitotic stage 10–11 anthers. *Arrows* in the *pirl1/PIRL1*;*pirl9* anther indicate arrested microspores, which retain the large vacuoles characteristic of younger uninucleate microspores (Regan and Moffatt 1990), while phenotypically normal pollen segregating in the same anther are undergoing vacuolar breakdown. **d** Locule from a later mitotic stage anther. Some double mutants

(*arrows*) are becoming deformed; one still resembles an arrested vacuolated microspore. **e, i** Locules from maturing stage 12–13 anthers; double mutants are empty, deformed, and clearly inviable (e.g. **e**, *arrow*). **j–m** TEM of arrested *pirl1*;*pirl9* microspores within *pirl1/PIRL1*;*pirl9* anthers. **j** A developmentally arrested double-mutant microspore (at center-left) in a mitotic stage anther, still featuring a large vacuole, the characteristic three-lobed morphology of uninucleate microspores from younger anthers, and an abnormally thin intine layer. Neighboring grains are phenotypically normal *PIRL1*;*pirl9* pollen segregating within the locule. *Arrows* indicate intine. **k** Phenotypically normal pollen in a stage 12 anther, illustrating appearance after characteristic vacuolar fission. **l** An arrested *pirl1*;*pirl9* microspore from same locule as **k**, illustrating the remnant large vacuole. Cytoplasm has begun degenerating and appears grainy. **m** A maturing post-mitotic anther with normal pollen (*top*) and an aborted *pirl1*;*pirl9* mutant (*bottom*). *Scale bars* **j–l** 5 μm; **m** 10 μm

differences in size and morphology were detected in anthers during stage 10 when microspores normally undergo the first pollen mitosis and initiate vacuolar fission (Regan and Moffatt 1990; Sanders et al. 1999; Yamamoto et al. 2003). First, double mutants appeared smaller than phenotypically normal pollen segregating within the same anthers, and they retained the large vacuole, single large nucleus, and homogenous toluidine blue staining characteristic of uninucleate microspores in stage nine anthers

(Regan and Moffatt 1990; Sanders et al. 1999). As anthers approached maturity, normal pollen continued to enlarge while double mutants remained significantly smaller, lost cytoplasm, and became increasingly misshapen (Fig. 5d, e). Similar developmental arrest was observed with TEM (Fig. 5j–m), which showed arrested microspores that failed to undergo vacuolar fission and appeared to have thin intine compared to normal mitotic pollen segregating within the same locule. Following developmental arrest, cytoplasm in

double mutants appeared grainy, detached, and eventually degenerated as anther development progressed (Fig. 5l, m).

To more precisely define the developmental arrest of *pirl1;pirl9* pollen and further confirm that observed defects parallel the segregation of the double-mutant genotype, developing *pirl1;pirl9* pollen segregating in tetrads in a *qrt1* background were stained with DAPI and observed at different developmental stages. Representative tetrads are shown in Fig. 6. In tetrads from stage 9 anthers, nuclear staining patterns were indistinguishable between double-mutants and normal sibling microspores segregating within the same tetrad (Fig. 6f). However, as anther development progressed to the mitotic stages the double-mutant phenotype consistently became apparent. Double mutants from bicellular-stage anthers remained uninucleate, while normal pollen segregating within the same tetrads featured both a large vegetative nucleus and a clear, brightly focused generative nucleus (Fig. 6g, h). Coinciding with these differences in DAPI staining, mutant members of these bicellular-stage tetrads also appeared slightly smaller than their phenotypically normal siblings, reflecting very recent growth arrest (evident in bright field images; Fig. 6b, c). This size difference became more pronounced in early tricellular stage tetrads as normal pollen continued to increase in size and approached maturity, while mutants began losing nuclear content and becoming distorted (Fig. 6d, i). Mutants in tetrads with mature tricellular pollen shortly before anthesis appeared shrunken and lacked DAPI staining. Altogether, in *pirl1/PIRL1;pirl9* tetrads segregating for the *pirl1;pirl9* genotype, no mutant microspores were observed

beyond the uninucleate stage ($n > 198$). Therefore, *PIRL1* and *PIRL9* are first required in developing pollen during anther stage 9–10, after exine has been established and microspores become vacuolated, but before mitosis and differentiation into functional tricellular pollen are initiated.

During normal pollen development, a transient callose disk forms between the vegetative nucleus and newly formed generative nucleus just after the first pollen mitosis (Park and Twell 2001). We used aniline blue, a fluorescent callose-binding stain, to determine whether such a disk forms in *pirl1;pirl9* double mutants. Results of representative tetrads observed at just this point in development are shown in Fig. 7. We consistently did not observe callose walls in double-mutant pollen, while the walls were clearly visible in mitotically competent normal pollen segregating within the same tetrads (Fig. 7e–h). As with DAPI staining, these internal differences became evident just at the point in development at which size differences between double mutant and normal pollen became apparent (Fig. 7a–d, bright field images), suggesting that developmental arrest occurs in *pirl1;pirl9* microspores just prior to the first pollen mitosis.

Discussion

A new class of LRRs associated with pollen development

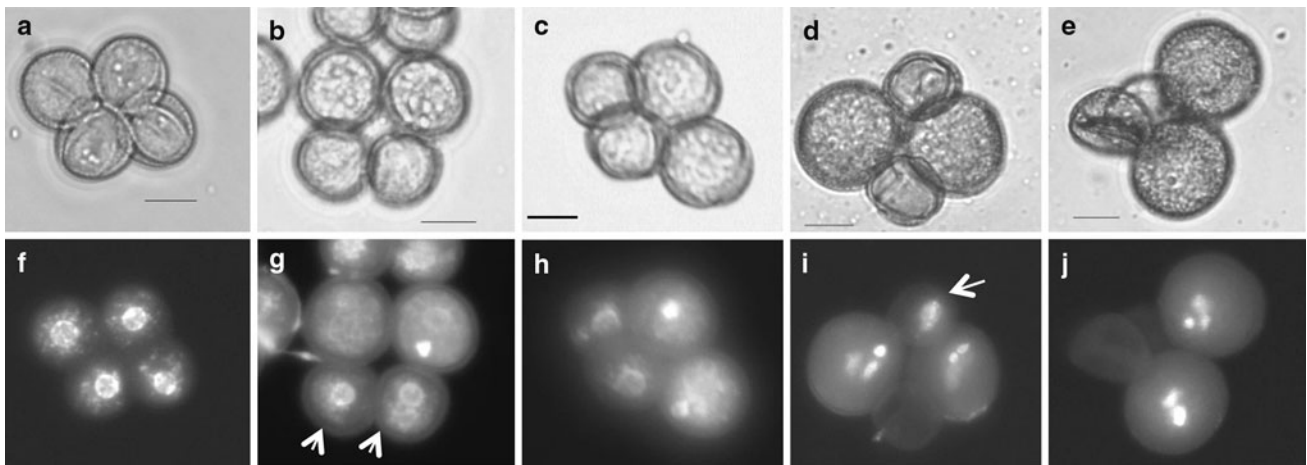*PIRL1* and *PIRL9* are members of a novel, plant-specific class of LRR proteins whose leucine-rich domains are

Fig. 6 Developmental arrest of mutant microspores before the first pollen mitosis. Tetrads produced by *qrt1;pirl1/PIRL1;pirl9* plants (segregating for 50% *pirl1;pirl9* double mutants) were stained with DAPI, and viewed with phase contrast (**a–e**) or fluorescence (**f–j**). Representative tetrads from anthers at different developmental stages are shown. **a, f** Uninucleate microspores shortly before pollen mitosis I; double mutants are not yet distinguishable by size or nuclear content. **b, c, g, h** Tetrads from anthers at the bicellular stage. Double

mutants (*white arrows*) are now distinguishable, appearing slightly smaller in tetrads viewed with phase contrast (**b, c**) and resembling the DAPI staining characteristic of uninucleate microspores (**g, h**). **d, i** Tetrad with two larger pollen at the early trinucleate stage. Double mutants remain arrested at microspore size, one with a single, smeared DAPI pattern (*arrow*), one lacking DNA. **e, j** A tetrad from a maturing anther, with viable pollen at the late trinucleate stage and double-mutant pollen that now lack DAPI staining
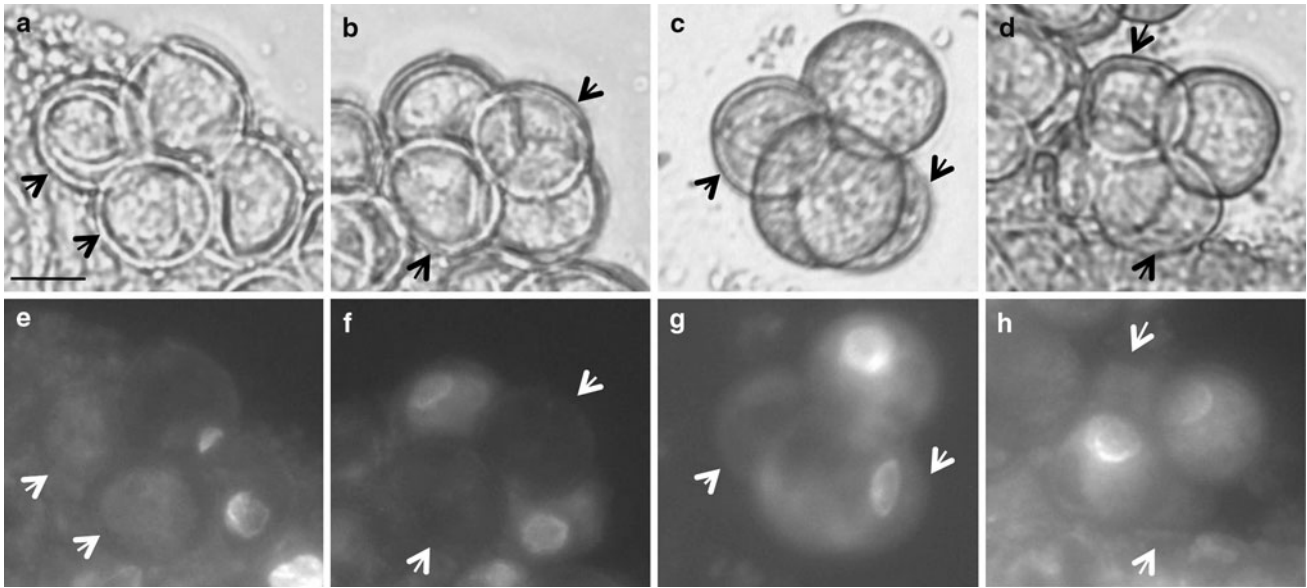
Fig. 7 Pre-mitotic arrest of *pirl1*;*pirl*9 microspores visualized by aniline blue staining. Tetrads produced by *qrt1*:*pirl1*/*PIRL1*;*pirl9* plants (segregating for 50% *pirl1*:*pirl9* double mutants) were stained with aniline blue and visualized at the start of the binucleate stage to assess formation of the transient callose disks that form between pollen nuclei after pollen mitosis I (Park and Twell 2001). **a–d** Representative bicellular stage tetrads just after pollen mitosis I, viewed with phase contrast. **e–h** The same tetrads as **a–d**, viewed with fluorescence. Callose disks can be seen in two phenotypically normal bicellular pollens in each tetrad. *Arrows* indicate positions of double-mutant microspores, which lack staining and appear very slightly smaller than normal siblings, reflecting recent developmental arrest. All pictures are at the same magnification; *bar* 10 μM

related to those of Ras-group LRRs that function in cell signaling and gene regulation in animals. Here, we have shown that *PIRL1* and *PIRL9* are essential for the differentiation of microspores into pollen, a process specific to plant development. Segregation of defective pollen in *qrt1* tetrads demonstrated that the *pirl1*:*pirl9* phenotype arises after meiosis, thus indicating that these genes are active and essential during the haploid phase. This was further confirmed by the lack of any obvious defects in early microspores, which were indistinguishable from developmentally normal microspores segregating within the same anthers. Mutation of both *pirl1* and *pirl9* consistently caused developmental arrest at the late microspore stage, just before the first pollen mitosis.

Different types of LRR proteins, in several model species, have been previously associated with pollen development. Examples include LRR-receptor kinases such as tomato LePRK1, 2, and 3, as well as related proteins in maize, petunia, and Arabidopsis (Kim et al. 2002; Muschietti et al. 1998). A secreted pollen-specific LRR, SHY, was identified in petunia and tomato, and has been implicated in signaling important for pollen tube growth, perhaps serving as a ligand for PRK receptors (Guyon et al. 2004; Tang et al. 2004). Another class of pollen-specific LRRs identified in tomato, maize, and Arabidopsis, the PEX proteins, share conserved LRR domains and are associated with pollen tube cell walls (Stratford et al. 2001). All of these examples of pollen-related LRRs are

expressed late in pollen development and are primarily associated with pollen tube elongation and guidance (Kim et al. 2002; Guyon et al. 2004). PIRL1 and PIRL9 represent a new class of pollen-associated LRRs critical at a much earlier point in pollen development.

The *PIRL1* and *PIRL9* genes form a related gene pair within the Arabidopsis *PIRL* family, and our results indicate that they are functionally redundant. As single mutations, *pirl1* and *pirl9* alleles showed normal transmission and resulted in no obvious developmental phenotypes, except for a slight increase in pollen inviability that was only ∼1–7% above the frequency observed for wild type (Fig. 3). Disruption of both genes together, however, had a highly penetrant impact on pollen development, causing consistent arrest of microspores. There may be a slight asymmetry in the redundant relationship between these two *PIRL*s: *pirl9* single mutants produced a slightly higher percentage of inviable pollen. However, that frequency, approximately 6%, was little above background and ultimately had no discernible effect on observed transmission frequency.

A number of forward genetic approaches have been employed to identify genes involved in pollen development (Feldmann et al. 1997; Boavida et al. 2009; Procissi et al. 2001; Johnson et al. 2004; Howden et al. 1998; McCormick 2004). *PIRL1* and *PIRL9* would not be identified in such screens due to their genetic redundancy. Furthermore, microarrays have been employed to identify genes

important in pollen development (Pina et al. 2005; Honys and Twell 2004; da Costa-Nunes and Grossniklaus 2003). While microarray data indicate expression of both of these genes in anthers and developing pollen (Zimmermann et al. 2004; Winter et al. 2007; https://www.genevestigator.ethz.ch; http://bar.utoronto.ca/efp/cgi-bin/efpWeb.cgi), an essential role in pollen development might not be predicted a priori from those data because *PIRL1* and *PIRL9* expression is not pollen-specific. RNA blotting, RT-PCR, and microarray data indicate that both genes are also widely expressed in the sporophyte (Forsthoefel et al. 2005; Zimmermann et al. 2004; https://www.genevestigator.ethz.ch). The results reported here therefore provide an example of how in-depth genetic and reverse-genetic investigation of specific gene families can contribute to functional genomic studies of pollen development, as well as other plant developmental processes.

Features of the *pirl1*;*pirl9* mutant phenotype

Several features of the *pirl1*;*pirl9* phenotype are notable. The first is the consistent early stage of developmental arrest. This early arrest accounts for the morphological severity and the high frequency of transmission failure: pre-mitotic arrest does not allow for production of sperm nuclei and development of functional pollen. Many male gametophyte mutations identified to date disrupt early pollen development, but do not result in consistent pre-mitotic arrest. For example, *sidecar pollen*, *gem*, *duo*, *mud*, and *gum* mutations affect pollen mitoses, post-mitotic cell fate, or organization of the male germ unit, but all allow development to progress to the bicellular stage or beyond (Chen and McCormick 1996; Park et al. 1998; Lalanne and Twell 2002; Durbarry et al. 2005; Brownfield et al. 2009; Borg et al. 2009). Other mutants, such as *raring-to-go* and many of the *hapless* mutants, affect later pollen stages, causing abnormal pollen tube germination, growth or guidance (Johnson and McCormick, 2001; Johnson et al. 2004). Some previously identified mutations that do disrupt earlier (microspore) development do not disrupt gametophytic gene activity, but rather are male-sterile mutations that result in even earlier defects in all microspores of the mutant anther, regardless of microspore genotype (e.g., Regan and Moffatt 1990; Taylor et al. 1998). These are therefore genetically distinct from the *pirl* mutations described here.

We observed a lack of vacuolar fission and a reduced intine layer in arrested double-mutant microspores from mitotic anthers. However, we do not necessarily propose a causal relationship between either of these features and developmental arrest: either of these could be consequences rather than primary causes of arrest. Based on both histology and TEM, it seems likely that *pirl1*;*pirl9*

developmental arrest occurs prior to the break up of the vacuole that normally accompanies mitotic stages in Arabidopsis anthers (Yamamoto et al. 2003; Regan and Moffatt 1990). Likewise, it is possible that the observed reduced intine could be an early consequence, rather than source, of developmental arrest in *pirl1*;*pirl9* microspores, which initiate internal degeneration after development halts (a process that has been observed with some other pollen-lethal knockout mutants; Leon et al. 2007; Lee et al. 2008). It is difficult to determine the chronological relationship between ultrastructural features in the mutant microspores, given the technical limitations of TEM for viewing large numbers of segregating pollen during the transient developmental time window between the appearance of phenotypic differences and the rapid degeneration of the cytoplasm.

Another notable feature of the *pirl1*;*pirl9* phenotype is that it is specific to development of the male gametophyte; the double-mutant allele combination was transmitted normally through the female gametophyte in reciprocal crosses. Similar male-specific gametophytic lethality has been observed for other Arabidopsis mutants, such as (for example) MAP3Kε knockout mutants (Chaiwongsar et al. 2006) and the *duo pollen* mutants (Durbarry et al. 2005). In fact, a large percentage of gametophyte mutants identified in forward screens were defective specifically in the male gametophyte (Boavida et al. 2009; Procissi et al. 2001; Johnson et al. 2004). Together, these results indicate, not surprisingly, that there are substantial differences in the genetic requirements for Arabidopsis male and female gametophyte development. The *pirl1*;*pirl9* knockout phenotype is consistent with this and indicates that male-specific gene functions contribute to microspores and early stages of pollen differentiation, not just to later, more obvious pollen-specific processes such as pollen tube growth and guidance.

The *PIRL*s may contribute to one of several cellular processes critical for the dynamic development of microspores and differentiation of pollen. For example, they may be involved in early events in mitosis or initiation of vacuolar break up. A role in microspore growth does not seem likely since mutant microspores appear to grow normally until just prior to pollen mitosis I, and they undergo proper vacuolization during the pre-mitotic growth stage (Regan and Moffatt 1990). Given the consistent, specific timing of arrest of *pirl1*;*pirl9* microspores, it is possible that these *PIRL* genes may have a regulatory function in the microspore–pollen transition because a more general housekeeping function might be expected to result in earlier microspore growth defects and/or more variable timing of arrest. A regulatory function, either in signaling or gene regulation, would be consistent with known functions for animal Ras-group LRRs (Dai et al.

2006; Sieburth et al. 1998; Li et al. 2000; Jeong et al. 2009; Lee et al. 2004; Cutler et al. 1992). However, we cannot entirely rule out that *PIRL*s take part in a fundamental cellular process that somehow has an acute impact on microspore development just before pollen mitosis I.

While our results indicate that *PIRL1* and *PIRL9* first become essential just prior to pollen mitosis I, they do not rule out additional roles for these genes later in development, either in pollen or in the sporophyte. In fact, their expression in mitotic pollen as well as sporophytic organs (Forsthoefel et al. 2005; Zimmermann et al. 2004; Winter et al. 2007; http://bar.utoronto.ca/efp/cgi-bin/efpWeb.cgi) suggests that both of these *PIRL*s may have additional functions later in plant development. This is not surprising: while the Arabidopsis pollen transcriptome is relatively rich in pollen-specific mRNAs (Honys and Twell 2003; 2004), it still shares at least 60% overlap with the sporophyte transcriptome, including some genes of developmental significance (Borg et al. 2009; Honys and Twell 2003). The pollen lethality of the *pirl1;pirl9* double-knockout phenotype prevents straightforward genetic dissection of potential additional roles in the sporophyte. Future investigation of *PIRL1* and *PIRL9* using inducible knockdowns in the sporophyte is one promising strategy to investigate this.

References

Alexander MP (1969) Differential staining of aborted and non-aborted pollen. Stain Technol 41:117–122

Alonso JM, Stepanova AN, Leisse TJ, Kim CJ, Chen H, Shinn P, Stevenson DK, Zimmerman J, Barajas P, Cheuk R, Gadrinab C, Heller C, Jeske A, Koesema E, Meyers CC, Parker H, Prednis L, Ansari Y, Choy N, Deen H, Geralt M, Hazari N, Hom E, Karnes M, Mulholland C, Ndubaku R, Schmidt I, Guzman P, Aguilar-Henonin L, Schmid M, Weigel D, Carter DE, Marchand T, Risseeuw E, Brogden D, Zeko A, Crosby WL, Berry CC, Ecker JR (2003) Genome-wide insertional mutagenesis of *Arabidopsis thaliana*. Science 301:653–657

Baez JM, Riveros M, Lehnback C (2002) Viability and longevity of pollen of *Notofagus* species in south Chile. N Z J Bot 40:671–678

Belkhadir Y, Subramaniam R, Dangl JL (2004) Plant disease resistance protein signaling: NBS-LRR proteins and their partners. Curr Opin Plant Biol 7:391–399

Boavida LC, Shuai B, Yu HJ, Pagnussat GC, Sundaresan V, McCormick S (2009) A collection of Ds insertional mutants associated with defects in male gametophyte development and function in *Arabidopsis thaliana*. Genetics 181:1369–1385

Borg M, Brownfield L, Twell D (2009) Male gametophyte development: a molecular perspective. J Exp Bot 60:1465–1478

Brownfield L, Hafidh S, Durbarry A, Khatab H, Sidorova A, Doerner P, Twell D (2009) Arabidopsis DUO POLLEN3 is a key regulator of male germline development and embryogenesis. Plant Cell 21:1940–1956

Buchanan SG, Gay NJ (1996) Structural and functional diversity in the leucine-rich repeat family of proteins. Prog Biophys Mol Biol 65:1–44

Chaiwongsar S, Otegui MS, Jester PJ, Monson SS, Krysan PJ (2006) The protein kinase genes MAP3K epsilon 1 and MAP3K epsilon 2 are required for pollen viability in *Arabidopsis thaliana*. Plant J 48:193–205

Chen YC, McCormick S (1996) Sidecar pollen, an *Arabidopsis thaliana* male gametophytic mutant with aberrant cell divisions during pollen development. Development 122:3243–3253

Claudianos C, Campbell HD (1995) The novel flightless-I gene brings together two gene families, actin-binding proteins related to gelsolin and leucine-rich-repeat proteins involved in Ras signal transduction. Mol Biol Evol 12:405–414

Cushing DA, Forsthoefel NR, Gestaut DR, Vernon DM (2005) Arabidopsis emb175 and other ppr knockout mutants reveal essential roles for pentatricopeptide repeat (PPR) proteins in plant embryogenesis. Planta 221:424–436

Cutler ML, Bassin RH, Zanoni L, Talbot N (1992) Isolation of rsp-1, a novel cDNA capable of suppressing v-Ras transformation. Mol Cell Biol 12:3750–3756

da Costa-Nunes JA, Grossniklaus U (2003) Unveiling the gene-expression profile of pollen. Genome Biol 5:205

Dafini A, Devan P, Husband B (2005) Practical pollination biology. Enviroquest Ltd, Canada, p 590

Dai P, Xiong WC, Mei L (2006) Erbin inhibits RAF activation by disrupting the sur-8-Ras-Raf complex. J Biol Chem 281:927–933

De Smet I, Voss U, Jurgens G, Beeckman T (2009) Receptor-like kinases shape the plant. Nat Cell Biol 11:1166–1173

Dievart A, Clark SE (2004) LRR-containing receptors regulating plant development and defense. Development 131:251–261

Dong X, Hong Z, Sivaramakrishnan M, Mahfouz M, Verma DP (2005) Callose synthase (CalS5) is required for exine formation during microgametogenesis and for pollen viability in Arabidopsis. Plant J 42:315–328

Dougherty GW, Jose C, Gimona M, Cutler ML (2008) The Rsu-1-PINCH1-ILK complex is regulated by Ras activation in tumor cells. Eur J Cell Biol 87:721–734

Durbarry A, Vizir I, Twell D (2005) Male germ line development in Arabidopsis. duo pollen mutants reveal gametophytic regulators of generative cell cycle progression. Plant Physiol 137:297–307

Eitas TK, Dangl JL (2010) NB-LRR proteins: pairs, pieces, perception, partners, and pathways. Curr Opin Plant Biol 13(4): 472–477

Feldmann KA, Coury DA, Christianson ML (1997) Exceptional segregation of a selectable marker (KanR) in Arabidopsis identifies genes important for gametophytic growth and development. Genetics 147:1411–1422

Fluhr R (2001) Sentinels of disease. Plant resistance genes. Plant Physiol 127:1367–1374

Forsthoefel NR, Cutler K, Port MD, Yamamoto T, Vernon DM (2005) PIRLs: a novel class of plant intracellular leucine-rich repeat proteins. Plant Cell Physiol 46:913–922

Guan YF, Huang XY, Zhu J, Gao JF, Zhang HX, Yang ZN (2008) RUPTURED POLLEN GRAIN1, a member of the MtN3/saliva gene family, is crucial for exine pattern formation and cell integrity of microspores in Arabidopsis. Plant Physiol 147: 852–863

Guyon V, Tang WH, Monti MM, Raiola A, Lorenzo GD, McCormick S, Taylor LP (2004) Antisense phenotypes reveal a role for SHY, a pollen-specific leucine-rich repeat protein, in pollen tube growth. Plant J 39:643–654

Hellmann H, Estelle M (2002) Plant development: regulation by protein degradation. Science 297:793–797

Henry IM, Dilkes BP, Young K, Watson B, Wu H, Comai L (2005) Aneuploidy and genetic variation in the *Arabidopsis thaliana* triploid response. Genetics 170:1979–1988

Honys D, Twell D (2003) Comparative analysis of the Arabidopsis pollen transcriptome. Plant Physiol 132:640–652

Honys D, Twell D (2004) Transcriptome analysis of haploid male gametophyte development in Arabidopsis. Genome Biol 5:R85

Howden R, Park SK, Moore JM, Orme J, Grossniklaus U, Twell D (1998) Selection of T-DNA-tagged male and female gametophytic mutants by segregation distortion in Arabidopsis. Genetics 149:621–631

Jeong KW, Lee YH, Stallcup MR (2009) Recruitment of the SWI/SNF chromatin remodeling complex to steroid hormone-regulated promoters by nuclear receptor coactivator flightless-I. J Biol Chem 284:29298–29309

Johnson SA, McCormick S (2001) Pollen germinates precociously in the anthers of raring-to-go, an Arabidopsis gametophytic mutant. Plant Physiol 126:685–695

Johnson MA, von Besser K, Zhou Q, Smith E, Aux G, Patton D, Levin JZ, Preuss D (2004) Arabidopsis hapless mutations define essential gametophytic functions. Genetics 168:971–982

Johnson-Brousseau SA, McCormick S (2004) A compendium of methods useful for characterizing Arabidopsis pollen mutants and gametophytically-expressed genes. Plant J 39:761–775

Kajava AV (1998) Structural diversity of leucine-rich repeat proteins. J Mol Biol 277:519–527

Kim HU, Cotter R, Johnson S, Senda M, Dodds P, Kulikauska R, Tang W, Ezcura I, Herzmark P, McCormick S (2002) New pollen-specific receptor kinases identified in tomato, maize and Arabidopsis: the tomato kinases show overlapping but distinct localization patterns on pollen tubes. Plant Mol Biol 50:1–16

Kobe B, Deisenhofer J (1994) The leucine-rich repeat: a versatile binding motif. Trends Biochem Sci 19:415–421

Kobe B, Kajava AV (2001) The leucine-rich repeat as a protein recognition motif. Curr Opin Struct Biol 11:725–732

Krysan PJ, Young JC, Sussman MR (1999) T-DNA as an insertional mutagen in Arabidopsis. Plant Cell 11:2283–2290

Lalanne E, Twell D (2002) Genetic control of male germ unit organization in Arabidopsis. Plant Physiol 129:865–875

Lee YH, Campbell HD, Stallcup MR (2004) Developmentally essential protein flightless I is a nuclear receptor coactivator with actin binding activity. Mol Cell Biol 24:2103–2117

Lee Y, Kim ES, Choi Y, Hwang I, Staiger CJ, Chung YY (2008) The Arabidopsis phosphatidylinositol 3-kinase is important for pollen development. Plant Physiol 147:1886–1897

Leon G, Holuigue L, Jordana X (2007) Mitochondrial complex II is essential for gametophyte development in Arabidopsis. Plant Physiol 143:1534–1546

Letunic I, Doerks T, Bork P (2009) SMART 6: recent updates and new developments. Nucleic Acids Res 37:D229–D232

Li W, Han M, Guan KL (2000) The leucine-rich repeat protein SUR-8 enhances MAP kinase activation and forms a complex with Ras and Raf. Genes Dev 14:895–900

McCormick S (2004) Control of male gametophyte development. Plant Cell 16(Suppl):S142–S153

McHale L, Tan X, Koehl P, Michelmore RW (2006) Plant NBS-LRR proteins: adaptable guards. Genome Biol 7:212

Meinke DW (1995) Molecular genetics of plant embryogenesis. Annu Rev Plant Physiol Plant Mol Biol 46:369–394

Morillo SA, Tax FE (2006) Functional analysis of receptor-like kinases in monocots and dicots. Curr Opin Plant Biol 9:460–469

Morris ER, Walker JC (2003) Receptor-like protein kinases: the keys to response. Curr Opin Plant Biol 6:339–342

Muschietti J, Eyal Y, McCormick S (1998) Pollen tube localization implies a role in pollen-pistil interactions for the tomato receptor-like protein kinases LePRK1 and LePRK2. Plant Cell 10:319–330

Park SK, Twell D (2001) Novel patterns of ectopic cell plate growth and lipid body distribution in the Arabidopsis gemini pollen1 mutant. Plant Physiol 126:899–909

Park SK, Howden R, Twell D (1998) The *Arabidopsis thaliana* gametophytic mutation gemini pollen1 disrupts microspore polarity, division asymmetry and pollen cell fate. Development 125:3789–3799

Paxson-Sowders DM, Dodrill CH, Owen HA, Makaroff CA (2001) DEX1, a novel plant protein, is required for exine pattern formation during pollen development in Arabidopsis. Plant Physiol 127:1739–1749

Pina C, Pinto F, Feijo JA, Becker JD (2005) Gene family analysis of the Arabidopsis pollen transcriptome reveals biological implications for cell growth, division control, and gene expression regulation. Plant Physiol 138:744–756

Preuss D, Rhee SY, Davis RW (1994) Tetrad analysis possible in Arabidopsis with mutation of the QUARTET (QRT) genes. Science 264:1458–1460

Procissi A, de Laissardiere S, Ferault M, Vezon D, Pelletier G, Bonhomme S (2001) Five gametophytic mutations affecting pollen development and pollen tube growth in *Arabidopsis thaliana*. Genetics 158:1773–1783

Regan SM, Moffatt BA (1990) Cytochemical analysis of pollen development in wild-type Arabidopsis and a male-sterile mutant. Plant Cell 2:877–889

Sanders PM, Bui AQ, Weterings K, McIntire KN, Hsu YC, Lee PY, Truong MT, Beals TP, Goldberg RB (1999) Anther developmental defects in *Arabidopsis thaliana* male-sterile mutants. Sex Plant Reprod 11:297–322

Sieburth DS, Sun Q, Han M (1998) SUR-8, a conserved Ras-binding protein with leucine-rich repeats, positively regulates Ras-mediated signaling in *C. elegans*. Cell 94:119–130

Somers DE, Fujiwara S (2009) Thinking outside the F-box: novel ligands for novel receptors. Trends Plant Sci 14:206–213

Sternberg PW, Alberola-Ila J (1998) Conspiracy theory: RAS and RAF do not act alone. Cell 95:447–450

Stratford S, Barne W, Hohorst DL, Sagert JG, Cotter R, Golubiewski A, Showalter AM, McCormick S, Bedinger P (2001) A leucine-rich repeat region is conserved in pollen extensin-like (Pex) proteins in monocots and dicots. Plant Mol Biol 46:43–56

Sussman MR, Amasino RM, Young JC, Krysan PJ, Austin-Phillips S (2000) The Arabidopsis knockout facility at the University of Wisconsin-Madison. Plant Physiol 124:1465–1467

Tang W, Kelley D, Ezcurra I, Cotter R, McCormick S (2004) LeSTIG1, an extracellular binding partner for the pollen receptor kinases LePRK1 and LePRK2, promotes pollen tube growth in vitro. Plant J 39:343–353

Tax FE, Vernon DM (2001) T-DNA-associated duplication/translocations in Arabidopsis. Implications for mutant analysis and functional genomics. Plant Physiol 126:1527–1538

Taylor PE, Glover JA, Lavithis M, Craig S, Singh MB, Knox RB, Dennis ES, Chaudhury AM (1998) Genetic control of male fertility in *Arabidopsis thaliana*: structural analyses of postmeiotic developmental mutants. Planta 205:492–505

Trump BF, Smuckler EA, Benditt EP (1961) A method for staining epoxy sections for light microscopy. J Ultrastruct Res 5:343–348

Vernon DM, Forsthoefel NR (2002) Leucine-rich repeat proteins in plants: diverse roles in signaling and development. In: Pandali SG (ed) Research signpost: recent research developments in plant biology, pp 202–214

Vernon DM, Meinke DW (1994) Embryogenic transformation of the suspensor in twin, a polyembryonic mutant of Arabidopsis. Dev Biol 165:566–573

Vernon DM, Hannon MJ, Le M, Forsthoefel NR (2001) An expanded role for the TWN1 gene in embryogenesis: defects in cotyledon pattern and morphology in the twn1 mutant of Arabidopsis (Brassicaceae). Am J Bot 88:570–582

Winter D, Vinegar B, Nahal H, Ammar R, Wilson GV et al (2007) An electronic fluorescent pictograph browser for exploring and analyzing large-scale biological data sets. PLoS One 2:e718

Yamamoto Y, Nishimura M, Hara-Nishimura I, Noguchi T (2003) Behavior of vacuoles during microspore and pollen development in *Arabidopsis thaliana*. Plant Cell Physiol 44:1192–1201

Zimmermann P, Hirsch-Hoffmann M, Hennig L, Gruissem W (2004) GENEVESTIGATOR. Arabidopsis microarray database and analysis toolbox. Plant Physiol 136:2621–2632